RF pulse design by optimal control with physical constraints

Armin Rund[1,2], Christoph Stefan Aigner[3], Karl Kunisch[1], and Rudolf Stollberger[2,3]

[1]*Institute for Mathematics and Scientific Computing, University of Graz, Graz, Austria,* [2]*BioTechMed Graz, Graz, Austria,* [3]*Institute of Medical Engineering, Graz University of Technology, Graz, Austria*

Synopsis

The design of customized RF pulse and slice selective gradient shapes gives rise to an optimal control problem for the Bloch equation with different inequality constraints. A state-of-the-art method of optimal control is designed especially for this problem class. The optimization model and method is applied to recent test examples. The results are validated on a 3T scanner with phantom and in vivo measurements.

Purpose

Optimal control based design of RF pulses in MRI was successfully applied to e.g. inversion[1], robust spatial spectral[2], or parallel transmission[3]. The purpose of this work is to extend optimal control formulations for joint design of customized RF pulse and slice selective gradient shape by inclusion of different constraints. Instead of the common least-square type performance index we add constraints to model the slice profile accuracy (magnitude and phase) and MR hardware restrictions (peak B1, peak gradient and peak slew rate). A state-of-the-art mathematical optimization method for constrained optimal control of the spin domain Bloch equation[4] is introduced and applied to the design of customized SMS pulse design.

Theory

An optimal control problem for the Bloch equations in the spin domain[4] with Cayley-Klein parameters α, β is formulated. The controls are the RF pulse $B_1(t)$ and the gradient slew rate $\dot{G}_\mathrm{s}(t)$. A desired profile (magnitude and phase) over the spatial coordinate z is prescribed at the terminal time T of the excitation or refocusing, together with maximum allowed errors e_*. For example, for a refocusing with perfect crusher gradients we prescribe in-slice $1-|\beta(z)|^2 \leq e_\mathrm{in}$, out-of-slice $|\beta(z)|^2 \leq e_\mathrm{out}$, and a in-slice phase constraint $|\varphi-\bar{\varphi}| \leq e_\mathrm{ph}$ with phase φ and mean phase $\bar{\varphi}$. Amplitude constraints $|B_1| \leq B_{1,\max}$, $|G_\mathrm{s}| \leq G_{\mathrm{s},\max}$, and $|\dot{G}_\mathrm{s}| \leq \dot{G}_{\mathrm{s},\max}$ are added to reflect the MR hardware restrictions. Since the profile accuracy is modeled as a constraint, the performance index can be customized according to the application problem. Here, we optimize for minimum SAR. The different inequality constraints are categorized into control constraints and state constraints[5], where the latter are penalized with a large even integer $p \gg 1$ in the objective using parameters $\mu_* > 0$

$$\min \sum_\mathrm{time} |B_1(t)|_2^2 + \mu_\mathrm{in} \sum_\mathrm{inslice} \left(\frac{1-|b(z,T)|^2}{e_\mathrm{in}} \right)^p + \mu_\mathrm{out} \sum_\mathrm{outslice} \left(\frac{|b(z,T)|^2}{e_\mathrm{out}} \right)^p + \mu_\mathrm{ph} \sum_\mathrm{slices} \sum_\mathrm{inslice} \left(\frac{\varphi-\bar{\varphi}}{e_\mathrm{ph}} \right)^p + \mu_\mathrm{g} \sum_\mathrm{time} \left(\frac{G_\mathrm{s}(t)}{G_{\mathrm{s},\max}} \right)^p$$

To handle the control constraints as hard constraints we set up a semismooth quasi-Newton method. The method is an extension of the trust-region semismooth Newton method[6]. Exact derivatives are formed via adjoint calculus[5] and matrix-free.

Methods

The proposed algorithm is implemented in MATLAB (The MathWorks, Inc, Natick, USA). The time discretization is fixed to a gradient raster time of 10µs. An iterative increase of p and a decrease of the parameters μ_* allows to find a minimum SAR solution. The method is tested on the examples given by the ISMRM Challenge 2015 test set[7] for a fixed pulse duration. Below we report the optimization results for a simultaneous multi-slice refocusing for a turbo spin echo sequence with a multiband factor of 10, a slice thickness of 2mm and a time-bandwidth product (TBP) of 3 starting from a PINS[8] initial. The constraints are a peak B1 of 18µT, a peak slew rate of 200mT/m/ms, a maximum refocusing error of 2%, and a maximum phase deviation of 0.01 radiant from the mean phase per slice. The optimized refocusing pulse is implemented on a 3T MR scanner (Magnetom Skyra, Siemens Healthcare, Erlangen, Germany) using a crushed spin echo sequence with a conventional superposed 90 degree SLR based excitation pulse. To validate the Bloch simulations, we acquired a high-resolution phantom scan (TR/TE=200/30ms, FOV=300x300mm, matrix=960×960) and an in-vivo scan (TR/TE=200/15ms, FOV=300x300mm, matrix=512×512). The second example shows the optimization with a multiband factor of 3 for a double-refocused diffusion sequence, using a slice thickness of 3mm and a TBP of 4. The constraints are as above, without the phase constraint. The out-of-slice error is doubled, which is nearly fulfilled by our initial guess from root-flipping[9].

Results and Discussion

Figure 1a shows the optimized real-valued RF pulse, slew rate and slice selective gradient shape. It exhibits 46.7% less SAR compared to the PINS initial while still fulfilling the requirements on the profile and the phase (assuming ideal crushers). Figure 2 shows the optimal result for the diffusion scenario. Here the optimization yields a complex-valued RF pulse. The SAR is reduced by 26.5% compared to the initial pulse from root-flipping. The phase is not part of the optimization. A scaling of the optimized B_1 to an exact flip angle of 180 leaves a SAR reduction of 40.8% resp. 15.1%. Figure 3 shows the reconstructed phantom and in vivo measurements using the optimized pulse from Figure 1. Both the phantom an in-vivo measurements show well defined slices and validate the Bloch simulations of Figure 1.

Conclusion

The presented approach demonstrates a general framework for the solution of optimal control methods for the Bloch equations with inequality constraints. By exploiting the inequality constraints, existing pulses are adapted iteratively to minimize a performance index. The performance index and the constraint parameters can be adapted to customize RF pulses and gradient shapes for a specific application.

Acknowledgements

supported by SFB F3209-18

References

1) M.S. Vinding, I.I. Maximov, Z. Tošner, N.C. Nielsen, Fast numerical design of spatial-selective RF pulses in MRI using Krotov and quasi-Newton based optimal control methods, J. Chem. Phys. 137 (5), 2012

2) M. Lapert, Y. Zhang, M.A. Janich, S.J. Glaser, D. Sugny, Exploring the physical limits of saturation contrast in magnetic resonance imaging, Sci. Rep. 2, 2012

3) W.A. Grissom, G.C. McKinnon, M.W. Vogel, Nonuniform and multidimensional Shinnar–Le Roux RF pulse design method, Magn. Reson. Med. 68 (3) 690–702, 2012

4) Pauly J, Le Roux P, Nishimura D, and Macovski A. Parameter relations for the Shinnar-Le Roux selective excitation pulse design algorithm. IEE Transactions on Medical Imaging 10(1), 1991

5) Tröltzsch F. Optimal control of partial differential equations. Graduate Studies in Mathematics 112, Amer. Math. Soc., 2010

6) Pieper K. Finite element discretization and efficient numerical solution of elliptic and parabolic sparse control problems. PhD Dissertation, TU Munich, April 2015

7) Grissom WA, Setsompop K, Hurley SA, Tsao J, Velikina JV and Samsonov AA. Advancing RF pulse design using an open-competition format: Report from the 2015 ISMRM challenge. Magn. Reson. Med., 2016

8) Norris DG, Koopmans PJ, Boyacioglu R and Barth M. Power Independent of Number of Slices (PINS) radiofrequency pulses for low-power simultaneous multislice excitation. Magn. Reson. Med. 66(5):1234–1240, 2011

9) Sharma A, Lustig M and Grissom WA. Root-flipped multiband refocusing pulses. Magn. Reson. Med. 75(1):227-237, 2015

Figures

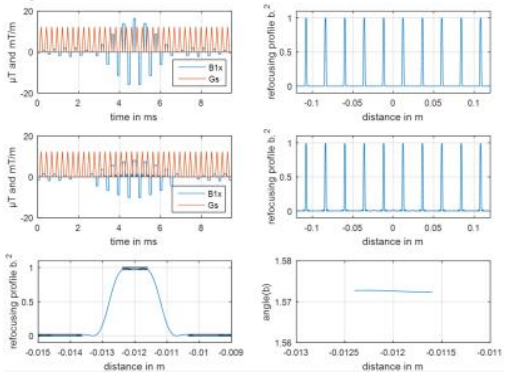

Figure 1: Comparison of the PINS pulse (row 1) with the optimized RF and slice selective gradient shape (row2) and the corresponding refocusing profiles from Bloch simulations. Row 3 shows a zoom into one slice of the optimized slice profile with corresponding phase distribution

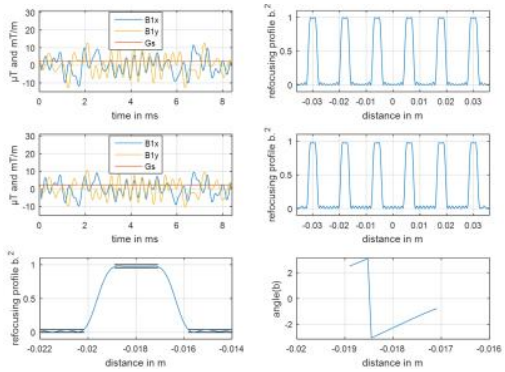

Figure 2: Comparison of the complex root-flipped pulse (row 1) with the optimized complex RF and slice selective gradient shape (row2) and the corresponding refocusing profiles from Bloch simulations. Row 3 shows a zoom into one slice of the optimized slice profile with corresponding phase (not part of the optimization here)

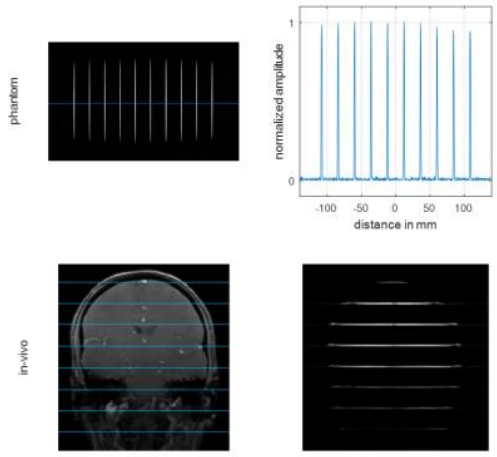

Figure 3: Reconstructed phantom and in vivo measurements of the pulse shown in Figure 1